J Mater Sci (2007) 42:4642–4649
DOI 10.1007/s10853-006-0519-4

Effect of microstructure on the modulus of PAN-based carbon fibers during high temperature treatment and hot stretching graphitization

Dongfeng Li · Haojing Wang · Xinkui Wang

Received: 2 March 2006 / Accepted: 6 June 2006 / Published online: 16 February 2007

Abstract The changes of microstructure and Young's modulus of PAN-based carbon fibers during the high temperature treatment (2400–3000 °C, stretching 0%) and hot stretching graphitization (0–5%, 2400 °C) were compared. It was observed that although the Young's modulus of the fibers could be increased by the two graphitization techniques, the microstructure parameters determined by X-ray diffraction were different for the same value of modulus. The relationship between microstructure and modulus showed that Young's modulus not only depended on the preferred orientation, but also related to the crystallite size (L_c and L_a) and shape (L_a/L_c). On the other hand, it was found that crystallite size of the fibers was mainly affected by heat treatment temperature and the crystallite shape could be altered by hot stretching graphitization. Further investigation indicated that the fibers were composed of turbostratic carbon structure even after heat treated to 3000 °C, which could be detected from the absence of 101 and 112 peaks in X-ray diffraction pattern, and the interlayer spacing (d_{002}) and preferred orientation (Z) were only 0.3430 nm and 14.71°, respectively.

D. Li (✉) · H. Wang · X. Wang
Key Laboratory of Carbon Materials, Institute of Coal Chemistry, Chinese Academy of Science, Taiyuan 030001, China
e-mail: lidf6304@126.com

D. Li
Graduate University of the Chinese Academy of Sciences, Beijing 100039, China

D. Li
Department of Chemistry, Xingtai College, Xingtai 054001, China

Introduction

Attributing to inherent structural characteristics, PAN-based carbon fibers have maintained their predominance as a reinforcing material in the present. Their high specific modulus and high specific strength, combined with their lightweight, make these fibers attractive for high volume applications ranging from sporting goods to aircraft structures [1–4]. There is a wide variety of commercially available PAN-based carbon fibers suitable for many different end uses, and the fibers can be classified into standard, intermediate and high modulus according to the difference in Young's modulus.

It is well known that the graphitization process is one of the most basic and important methodologies in carbon science because this technology is a very powerful tool for modifying the property of carbon materials. For example, the Young's modulus of carbon fibers can be increased either by high temperature treatment or by hot stretching graphitization [5–7]. Since the properties of carbon fibers directly depend on the structure, the control of structure and the study on relationship between the structure and properties during graphitization have been extensively studied by a number of researchers [8–12]. Although many studies have been reported on the effects of processing on the structure and properties of carbon fibers, a comparison of the effects of heat treatment temperature and hot stretching on microstructure and modulus of PAN-based carbon fibers has not appeared yet in the literature. Moreover, as to the relationship between Young's modulus and microstructure, much of the earlier work mainly focused on the effects of degree of preferred orientation [13–15] and a well-established correlation between preferred orientation and Young's

modulus was discovered. However, very little deal with the effects of the crystallite size and shape on Young's modulus of the carbon fibers.

In the present paper, the evolution of microstructure of PAN-based carbon fibers in continuous graphitization, which conducted by high temperature treatment and hot stretching graphitization, was examined by wide angle X-ray diffraction and Raman spectroscopy. In particular, the relationship between Young's modulus and microstructure parameters such as the crystallite size and shape, as well as the degree of preferred orientation, in these graphitization processes was compared.

Experimental

Materials

All experiments in this study were performed on PAN-based carbon fibers (Torayca Co., Ltd. commercial product T300-3K, Japan), with typical values of 230 GPa and 3.53 GPa for Young's modulus and tensile strength, respectively. The density of as-received carbon fibers is 1.76 g/cm^3.

Graphitization

A graphitization furnace with a hot-zone length of 180 mm at 3000 °C was allowed the carbon fibers to subject to continuous graphitization processing. The experiments were carried out in argon atmosphere and the residence time in high temperature zone was about 20 s. During graphitization hot stretching was performed by stretching machines to control the speeds of fibers in both sides of the graphitization furnace. The percentage of stretching was defined as the following relationship:

$$S = (V_a - V_b) / V_b$$

Where V_a is the speed of fibers after graphitization, and V_b is the speed of fibers before graphitization.

High temperature treatment was conducted at temperature ranging from 2400 °C to 3000 °C and the percentage of stretching was 0%, in which the speeds of the fibers maintained the same in both side of the graphitization furnace. During hot stretching graphitization, the percentage of the stretching varied from 0% to 5% at 2400 °C.

Characterization

Mechanical properties were tested in the form of tows and measured by AG-1 type universal material tester (Shimadzu Co., Ltd., Japan), in which crosshead speed was 20 mm/min and gauge length was 20 cm, and the densities of the fibers samples were measured using the flotation technique. At least 10 filaments were tested, and the average value was reported.

The Raman scattering measurements were performed in a Raman spectrometer (Renishow, RM 1000) at room temperature under a nitrogen atmosphere, using a 514.5 nm line of an argon ion laser as the incident radiation. The Raman-scattered light was dispersed by an optical grid and detected by a CCD camera, and the instrument was calibrated against the Stokes Raman signal of pure Si at 520 cm^{-1} using a silicon wafer. The Raman spectrometer was operated in the continuous scanning mode with laser beam powers of 4 mW and exposure times of 30s. The laser spot diameter reaching the fiber surface was about 2 μm. Instrument control and spectra analysis were performed with the software packages Renishow WiRE and the spectral resolution was about 2 cm^{-1}.

X-ray diffraction (XRD) patterns of all samples were obtained in an X-ray diffractometer (Rigaku D/max-rA, CuKα, 0.15148 nm, 40 kV, 60 mA) using a fiber specimen attachment. Fiber bundles were arranged parallel to each other and examined in symmetric transmission. Measurements were made by performing equatorial scan (perpendicular to the fiber axis), meridian scan (parallel to the fiber axis), as well as azimuthal scan (rotating the fibers in the attachment) at the fixed Bragg position, respectively. Silicon was used as a standard for peak position and broadening correction.

The diffraction scan curve was fitted with software to get peak position and peak widths, and the structure parameters of all samples were obtained as follows: the 002 peak from equatorial scan was used to estimate the value of the average interlayer spacing, d_{002}, and the apparent crystallite thickness, L_c, whereas the 100 peak from meridian scan was used for the apparent layer-plane length parallel to the fiber axis, L_a, which was described as $L_{a\|}$ in some literatures [16–18]. The value of d_{002} was calculated using Bragg's law, and the crystallite size L_c and L_a were calculated using Scherrer's formula:

$$d_{002} = \frac{\lambda}{2 \sin \theta}$$

$$L = \frac{K\lambda}{\beta \mathrm{COS}\ \theta}$$

Where θ is the scattering angle, λ is the wavelength of the X-rays used, and β is the full width at half maximum intensity (FWHM). The form factor K is 0.9 for L_c, and 1.84 for L_a, respectively [16, 19].

The degree of preferred orientation of graphite layer planes parallel to the fiber axis was obtained from azimuthal scan at the fixed Bragg position of the 002 reflection. The angular dependence of the intensity relative to the fiber equator is directly proportional to the angular dependence of the layer plane normals, which also represent the angular dependence of the layer planes themselves relative to the fiber axis. The diffraction intensity is measured as a function of the fiber tilt in the symmetric transmission plane. The full width at half maximum intensity [FWHM], Z, is a commonly used as a measure of the graphite layer degree of orientation [7, 15]. Thus, approximately two-thirds of the graphite layer planes lie within (Z/2)° to either side of the fiber axis [20].

Results and discussion

Young's modulus changes

Figure 1(a) shows the effects of graphitization temperature from 2400 °C to 3000 °C with stretching 0% on carbon fibers Young's modulus. With the temperature increasing, the Young's modulus increases from 343 GPa at 2400 °C to 424 GPa at 3000 °C, which increased up to approximately 24%.

It is known that the Young's modulus can also be increased by hot stretching processing during graphitization. So that continuous hot stretching graphitization experiments were conducted at 2400 °C, in which only variation was percentage of stretching (from 0% to 5%), while other conditions were the same as that of high temperature treatment. As shown in Fig. 1(b), the Young's modulus of carbon fibers increases from 343 GPa in 0% to 403 GPa in 5%, which increased up to approximately 17.5%.

The results of the experiments display that both high temperature treatment and hot stretching graphitization show an approximately linear relationship between modulus and processing condition. In addition, it is found that the modulus is significantly affected by the stretching degree.

Raman spectroscopy analysis

Raman spectroscopy has been shown to be a powerful method for characterizing the structural perfection in

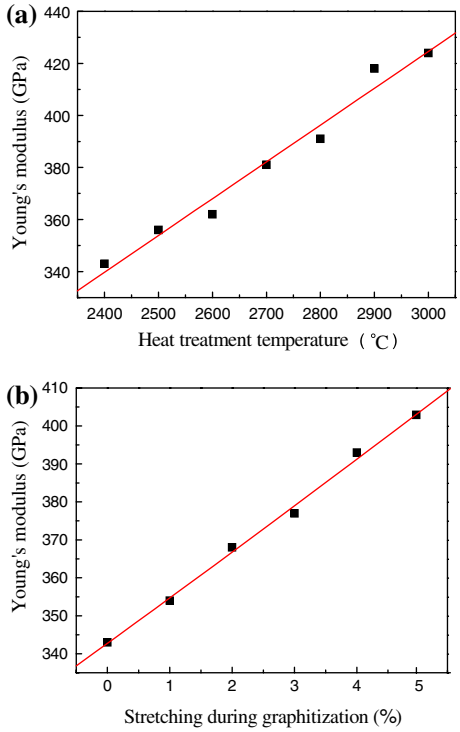

Fig. 1 Effects of heat treatment temperature and hot stretching on fibers Young's modulus: (**a**) hot stretching 0%; (**b**) heat treatment temperature at 2400 °C

carbonaceous materials [21, 22]. In order to get a general idea of the structural perfection within the fibers, Raman spectroscopy was utilized to characterize the changes which occur in the carbonaceous structures of these materials. In the first order spectrum (1000–2000 cm^{-1}), carbons mainly show two characteristic bands. The one is the Raman-allowed band at about 1580 cm^{-1} corresponding to an ideal graphitic lattice vibration mode with E_{2g} symmetry, often referring as the G-mode, and assigned to the "in-plane" displacement of the carbons strongly coupled in the hexagonal sheets. The another Raman active band is the disorder-induced band around 1360 cm^{-1} called the D-mode corresponding to a graphitic lattice vibration mode with A_{1g} symmetry, which is absent in the single crystal graphite. The disorder-induced band typically corresponds to an increase in the amount of unorganized carbon and a decrease in crystallite size. Figure 2 shows the first-order spectra of PAN-based carbon fibers heat treated at different temperatures. Even heat-treated at 3000 °C, the D band is clearly observed, indicating that the fibers still have disordered organization.

The degree of structural disorder of the fibers can be characterized by the ratio of integrated intensity of the disorder-induced band (D) to the Raman-allowed band

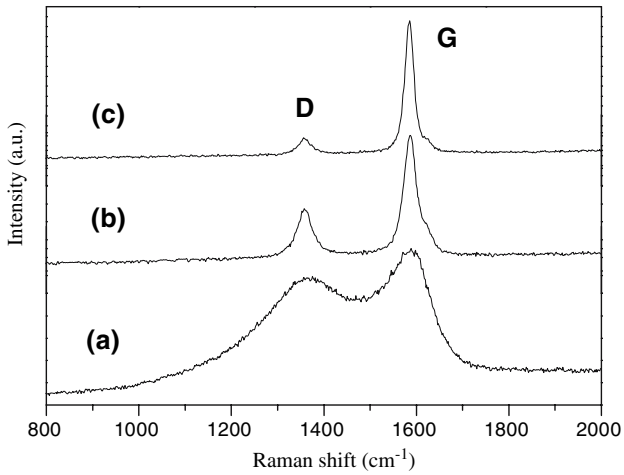

Fig. 2 Raman spectra of PAN-based carbon fibers heat-treated at different temperatures: (**a**) as-received (T300); (**b**) 2400 °C; (**c**) 3000 °C

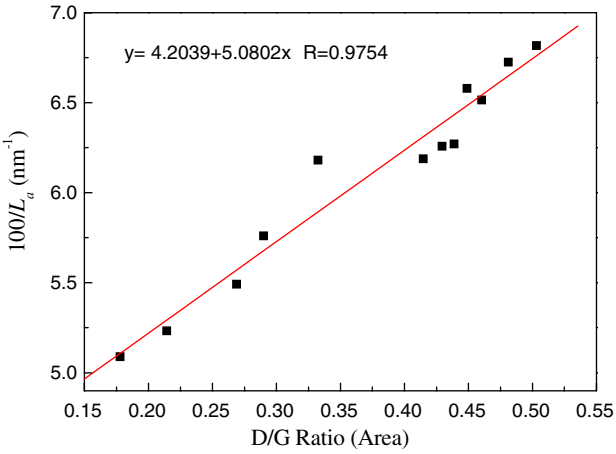

Fig. 4 The relationship between the D/G ratio and the inverse coherence length L_a which determined by X-ray diffraction

(G), which describes the amount of disorganized material in the material. As indicated in the Fig. 3(a), there is a large decrease in D/G during the heat treatment temperature from 2400 °C to 3000 °C, indicating that the crystal structure becomes more ordered. In hot stretching graphitization, however, the value of D/G in Fig. 3(b) shows a small decrease with increasing the percentage of stretching. In addition, according to Tuinstra et al. [21] the ratio of the integrated intensities of D/G was linearly related to the inverse of coherence length of crystallites (L_a) which determined by X-ray diffraction. As seen in Fig. 4, a similar result is likewise observed in this paper.

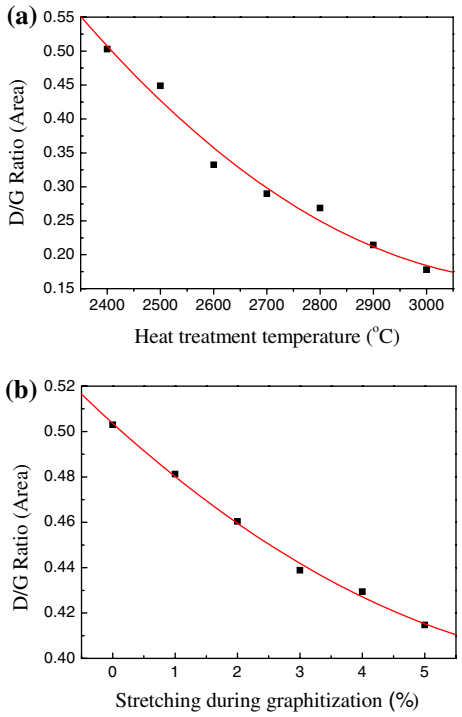

Fig. 3 Intensity ratio of D/G (area) as a function of (**a**) heat treatment temperature in stretching 0% and (**b**) stretching at 2400 °C

X-ray diffraction analysis

Microstructure changes in high temperature treatment

Figure 5 shows the XRD patterns of as-reserved carbon fibers heat-treated to 3000 °C, which are observed from equatorial, meridian and azimuthal scans, respectively.

Due to the anisotropy property of carbon fiber, there is an evident difference between equatorial and meridian scans. The appearance of 100 and 110 peaks and no 002 peak in the meridian scans indicate the preferred orientation of layer plane of graphite along fiber axis. However, from Fig. 6, it can be seen that the weak diffraction of 100 and 110 peaks still exist in equatorial scan whereas no such peaks are observed in high orientation graphite made from polyimide film [23], indicating that the layer planes are not highly aligned. In addition, when heat-treated to 3000 °C, 101 or 112 peaks of the XRD pattern for three-dimensional graphite structure does not appear.

The data of the microstructure parameters listed in Table 1 indicate that d_{002} decreases while L_a and L_c increases with the temperature increasing from 2400 °C to 3000 °C. The evolution of the microstructure (see Fig. 6) indicates that the degree of graphitization of carbon fibers can be significantly improved with the increasing temperature. The results can also

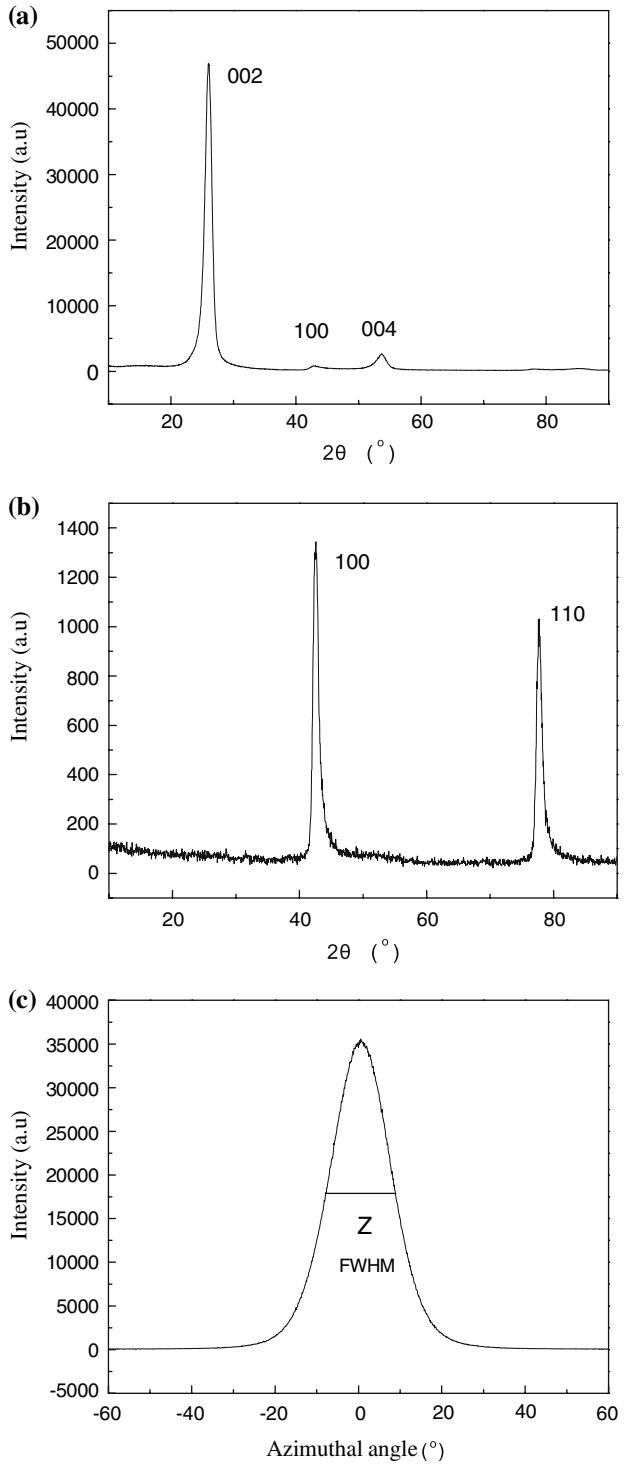

Fig. 5 X-ray diffraction patterns of as-received fibers heat-treated to 3000 °C: (**a**) equatorial scan; (**b**) meridian scan; (**c**) azimuthal scan

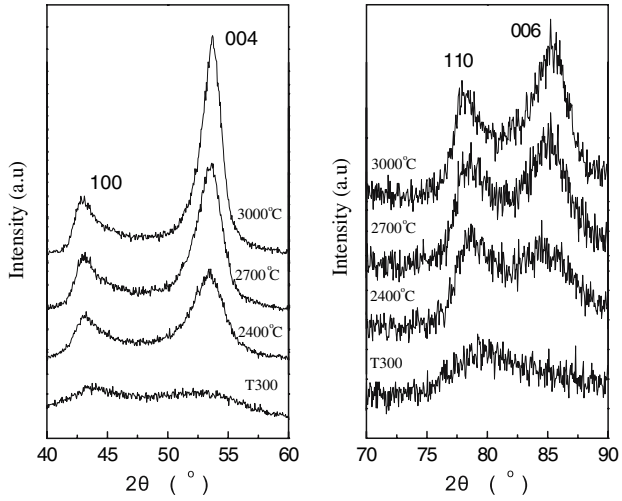

Fig. 6 X-ray diffraction patterns from equatorial scans at 2θ of 40–60° and 70–90° show the evolution of the structure

be confirmed by the image of High-resolution TEM in fibers fragment (see Fig. 7). Comparing with the as-received carbon fibers, the fibers heat-treated at 3000 °C show great increase in degree of graphitization and structural perfection. So far as the layer spacing is concerned, the layers remain only 0.3430 nm even after heat treated at 3000 °C, a value larger than that of ideal single graphite (0.3354 nm).

Crystallite shape was defined by Richards [24] as the ratio of the crystallite diameter to the crystallite height. As shown in Fig. 8(a), the crystallite shape in carbon fibers, L_a/L_c, decreases with increasing temperature, so the rate of growth in the apparent crystallite thickness is greater than that of the apparent layer-plane length parallel to the fiber axis from 2400 °C to 3000 °C. This further demonstrates that it is rather easy for the formation of π-bonds between layers versus the σ-band within layers, which resulting in a decrease of d-spacing.

The degree of preferred orientation of layer-planes parallel to the fiber axis, as determined by the full-width at half maximum (FWHM), Z, from azimuthal scan at the fixed Bragg position of the 002 reflection, is shown in Fig. 5(c). From the data listed in Table 1, we can see that the values of Z decrease with increasing temperature, for example, from 27.74° in as-reserved fibers, 19.08° at 2400 °C and 14.71° at 3000 °C. So the degree of preferred orientation in PAN-Based carbon fibers can be increased in graphitization with decrease in Z. However, compared with the highly oriented pyrolytic graphite (Z<5°), the PAN-based carbon fibers only have lower degree of preferred orientation even after heat treatment at 3000 °C.

Microstructure changes in hot stretching graphitization

Data presented in Table 1 display that with the percentage of hot stretching increasing from 0% to 5% during heat treatment temperature at 2400 °C, 2θ of

Table 1 X-ray diffraction structural parameters

HTT (°C)	Stretch %	2θ(002) (°)	FWHM 002	d_{002} (nm)	*Lc* (nm)	2θ(10) (°)	FWHM 100	*La*(10) (nm)	Z (°)
T300	–	24.88	4.87	0.3579	1.67	43.41	4.00	4.37	27.74
2400	0	25.76	2.00	0.3459	4.09	42.74	1.19	14.67	19.08
2500	0	25.80	1.82	0.3453	4.48	42.73	1.15	15.20	18.02
2600	0	25.84	1.65	0.3448	4.95	42.68	1.08	16.18	17.43
2700	0	25.89	1.53	0.3441	5.32	42.66	1.01	17.36	16.38
2800	0	25.91	1.40	0.3439	5.83	42.63	0.96	18.21	15.49
2900	0	25.92	1.30	0.3437	6.29	42.62	0.91	19.11	15.16
3000	0	25.98	1.19	0.3430	6.84	42.58	0.89	19.65	14.71
2400	1	25.77	1.98	0.3457	4.12	42.73	1.17	14.87	18.79
2400	2	25.79	1.92	0.3455	4.24	42.71	1.14	15.35	18.12
2400	3	25.79	1.89	0.3454	4.33	42.68	1.09	15.95	17.64
2400	4	25.80	1.88	0.3454	4.33	42.67	1.09	15.98	17.30
2400	5	25.80	1.87	0.3453	4.35	42.66	1.08	16.16	16.76

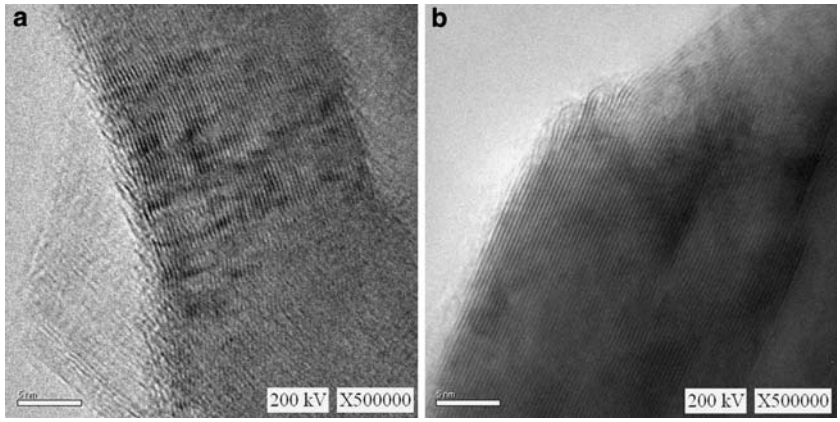

Fig. 7 High-resolution TEM lattice image in PAN-based carbon fiber fragment: (**a**) as-received carbon fiber; (**b**) heat treated at 3000 °C

002 peaks moves to higher angle and the average interlayer spacing, $d_{002,}$ has a small decrease from 0.3459 nm in 0% to 0.3453 nm in 5%. Meanwhile, L_c increases slightly from 4.09 nm to 4.35 nm whereas the L_a increases obviously from 14.67 to 16.16 nm. So the hot stretching graphitization can also enhance the degree of graphitization to some extent.

It is noticeable that the crystallite shape in carbon fibers may be changed by stretching graphitization at the given temperature. Figure 8(b) shows the effects of stretching on the crystallite shape L_a/L_c. The value of L_a/L_c increases from 3.59 to 3.71 with the percentage of hot stretching increasing from 0% to 5%. Therefore, the crystallite size is mainly dominated by heat treatment temperature while the crystallite shape can be changed by hot stretching graphitization.

Although the effect of hot stretching graphitization on crystallite size is not remarkable, it is found from Table 1 that this processing can effectively increase the degree of preferred orientation, therefore resulting in decrease of Z value from 19.08° in 0% to 16.76° in 5% stretching. The results may be attributed to the creep deformation and dislocation rearrangement of microcrystalline along the fiber axis during the hot stretching at high temperature, resulting in an increase of L_a and a decrease of Z.

Relationship between Young's modulus and microstructure

Young's modulus is the inherent property of carbon fibers and relates to microcrystalline structure. There are three theoretical models accounting for the relationship between microstructure and young's modulus, such as uniform stress, uniform strain and elastic unwrinkling. Although different models are used to describe the relationship between microstructure and modulus, it is common recognized that a well established correlation exists between preferred orientation and Young's modulus, namely, the smaller Z value, the higher modulus.

Figure 9 shows the relationship between degree of preferred orientation of graphite layer planes and the Young's modulus. It can be found that the Young's modulus increases with the decrease of preferred orientation parameter Z, regardless of processing technology used. However, when the same Young's modulus is attained either by high temperature treat-

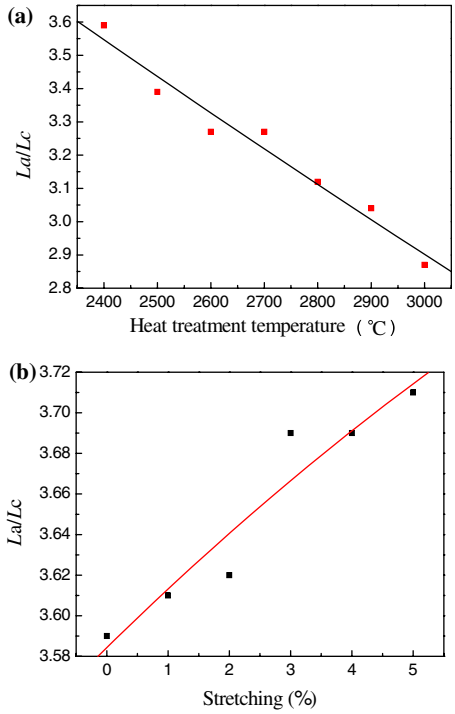

Fig. 8 Effects of (**a**) heat treatment temperature and (**b**) hot stretching on the crystallite shape L_a/L_c

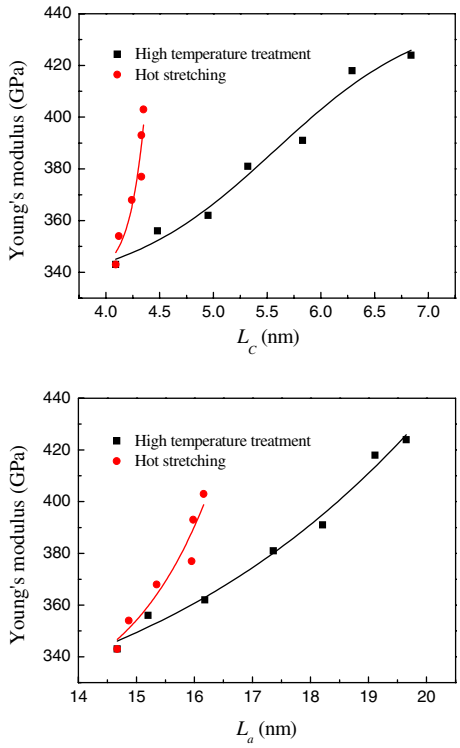

Fig. 10 Effects of crystallite size on fibers Young's modulus during graphitization

ment or by hot stretching graphitization, the preferred orientation parameter Z is not the same, the latter is larger.

Comparing parameters of microstructure listed in Table 1, it is evident that apart from the degree of preferred orientation, the crystallite size and shape in carbon fibers are also important factors on the Young's modulus. Figure 10 shows the changes of crystallite size against the modulus in two different graphitization techniques. It is found that the Young's modulus increases with increasing crystallite size (L_a and L_c). However, for the same modulus obtained from high temperature treatment and hot stretching graphitization, both the crystallite size and the degree of preferred orientation (see Fig. 9) are smaller, whereas the value of L_a/L_c is higher for hot stretching graphitization. Figure 11 shows the effects of L_a/L_c on fibers Young's modulus during hot stretching graphitization. It can be seen that the Young's modulus increases with

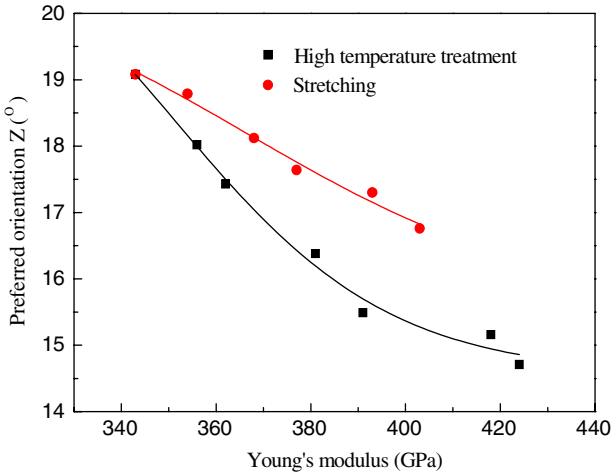

Fig. 9 Effects of the degree of preferred orientation on fibers Young's modulus during graphitization

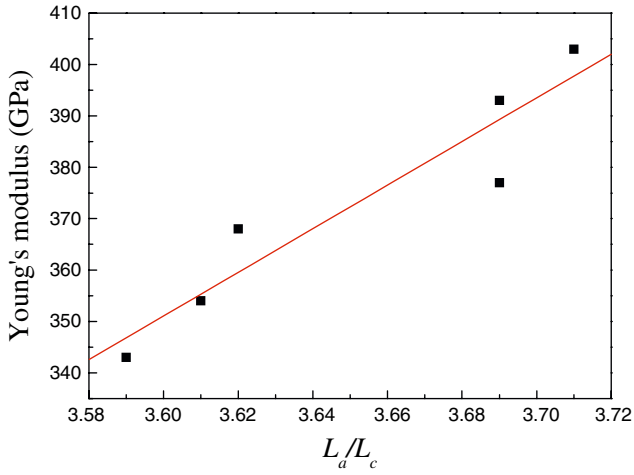

Fig. 11 Effects of L_a/L_c on fibers Young's modulus during hot stretching graphitization at 2400 °C

the increasing L_a/L_c at the given heat treatment temperature. So a significant increase in Young's modulus for hot stretching graphitization mainly comes from the increase in the degree of preferred orientation and L_a/L_c, particularly, from the increase of L_a.

Conclusions

In order to evaluate the effects of the microstructure of PAN-based carbon fibers in continuous graphitization on their Young's modulus and understand the microstructure–modulus relationship, two techniques are used to enhance the Young's modulus, one is the high temperature treatment; another is hot stretching graphitization. The results exhibit that these techniques have profound effects on the Young's modulus, and both the temperature and the stretching show an approximately linear relationship with the modulus.

Microstructure changes demonstrate the same trends for high temperature treatment and hot stretching graphitization. However, for the latter, the interlayer spacing and L_c increase slightly and a significant increase is found in L_a and preferred orientation. It is noticeable that the crystallite shape, L_a/L_c, increases with temperature and decreases with hot stretching, respectively.

The relationship between microstructure and modulus shows that the values of microstructure parameters, such as crystallite size and preferred orientation, are not the same by two techniques in achieving the same Young's modulus. It has been found that the Young's modulus of PAN-based carbon fibers not only depends on the degree of preferred orientation, but also relates to the crystallite size and shape.

Acknowledgements This research has been supported by funds from Chinese Academy of Science. The authors wish to thank Professor He Fu of the Key Laboratory of Carbon Materials, Institute of Coal Chemistry, Chinese Academy of Sciences, for useful advice, remarks and suggestions.

References

1. Chand S (2000) J Mater Sci 35:1303
2. Rubin L (1993) In: Buckley JD, Edie DD (eds) Carbon–carbon materials and composites. Noyes publications, New Jersey, p 267
3. Chung DDL (1994) In: Carbon fiber composites. Butterworth-Heinemann, Newton, p 81
4. Dorey G (1987) J Phys D: Appl Phys 20:245
5. Ozbek S, Isaac DH (1994) Mater Manuf Process 9:199
6. Ozbek S, Isaac DH (2000) Carbon 38:2007
7. Bacon R (1973) In: Walker PL Jr, Thrower PA (eds) Chemistry and physics of carbon, vol 9. Marcel Dekker, New York, p 1
8. Huang Y, Young RJ (1995) Carbon 33:97
9. Edie DD (1998) Carbon 36:345
10. Fitzer E (1989) Carbon 27:621
11. Endo M (1988) J Mater Sci 23:598
12. Johnson DJ, Tyson CN (1969) J Appl Phys 2:787
13. Kogure K, Sines G, Gerard LJ (1994) Carbon 32:715
14. Johnson DJ (1987) J Phys D: Appl Phys 20:286
15. Ogale AA, Lin C, Anderson DP, Kearns KM (2002) Carbon 40:1309
16. Johnson DJ (1980) Phil Trans R Soc Lond A 294:443
17. Johnson DJ (1987) In: Walker PL Jr, Thrower PA (eds) Chemistry and physics of carbon, vol 20. Marcel Dekker, New York, p 1
18. Ruland W (1968) In: Walker PL Jr (ed) Chemistry and physics of carbon, vol 4. Marcel Dekker, New York, p 1
19. Cuesta A, Dhamelincout P, Laureyns A, Martinez-Alonso, Tascon JMD (1998) J Mater Chem 8:2875
20. Jones SP, Fain CC, Fdid DD (1997) Carbon 35:1533
21. Tuinstra F, Koenig JL (1970) J Chem Phys 53:1126
22. Melanitis N, Tetlow PL, Galiotis C (1996) J Mater Sci 31:851
23. Murakami M, Nishiki N, Nakamura K, Ehara J, Okada H, Kouzaki T, Watanabe K, Hoshi T, Yoshimura S (1992) Carbon 30:255
24. Richards BP (1968) J Appl Crystallogr 1:35